Estimation precision of degree of polarization in the presence of signal-dependent and additive Poisson noises

Arnaud Bénière
arnaud.beniere@institutoptique.fr
Laboratoire Charles Fabry de l'Institut d'Optique, CNRS, Univ Paris-Sud, Campus Polytechnique, RD 128, 91127 Palaiseau, France
Thales Research and Technology - France, RD128, 91767 Palaiseau Cedex, France

François Goudail
francois.goudail@institutoptique.fr
Laboratoire Charles Fabry de l'Institut d'Optique, CNRS, Univ Paris-Sud, Campus Polytechnique, RD 128, 91127 Palaiseau, France

Mehdi Alouini
mehdi.alouini@thalesgroup.com
Thales Research and Technology - France, RD128, 91767 Palaiseau Cedex, France

Daniel Dolfi
daniel.dolfi@thalesgroup.com
Thales Research and Technology - France, RD128, 91767 Palaiseau Cedex, France

We address precision of estimation of the degree of polarization (DOP) from the orthogonal state contrast image (OSCI) in the presence of both signal-dependent Poisson noise due to useful signal, and additive Poisson noise due to dark current and / or background light. We determine the Cramer Rao Lower Bound and deduce from it figures of merit for DOP estimation. In particular, we show that the additive Poisson noise has larger influence on DOP estimation than on intensity estimation when light is highly polarized. [DOI: 10.2971/jeos.2008.08002]

Keywords: Polarization, noise in imaging systems, polarimetry

1 INTRODUCTION

Polarimetric imaging is an important tool for characterizing materials and observing contrasts that are not detectable in conventional intensity images. It has applications in remote sensing [1, 2], biomedical imaging [3, 4], optical coherence tomography [5], etc. A simple but efficient active polarimetric imaging mode consists in measuring the orthogonal state contrast image (OSCI) from two intensity measurements. The OSCI is an estimate of the degree of polarization (DOP) if the observed material is purely depolarizing, which is a reasonable assumption for natural materials observed in monostatic configuration [6]. We will make this assumption in the following of this paper. However, these intensity measurements are perturbed with noise, and its influence on DOP estimation must be studied. Such analyses have recently been done for Gamma noise [7], combined Poisson and speckle noise [8], and Gaussian noise [9].

We address in this paper the case where the two active intensity images used to build up the OSCI image are perturbed by the signal-dependent Poisson noise due to the useful signal and an additive Poisson noise that is independent of the useful signal. This latter can be due to background light, dark current or surrounding light which is reflected or backscattered by the scene and is considered as a passive contribution. This model has not yet been studied in the literature, whereas it can be relevant for example in infra-red imaging, where background noise is an important issue, in low flux images where dark current noise may not be negligible compared to useful signal, or in every active imaging system where a passive contribution due to other light sources will be encountered. The obtained results are thus useful for analyzing the impact of noise on DOP measurement by quantum detectors such as CCD.

This article is organized as follows. In Section 2, we describe the data model and discuss practical situations where it is relevant. In Section 3, we determine the Cramer-Rao Lower Bounds (CRLB) on estimation of the intensity and the DOP of a homogeneous sample in a OSCI and discuss their expressions relatively to previously published results. In Section 4, we analyze the physical meaning of these expressions of CRLB. We show that the additive Poisson noise has larger influence on DOP estimation than on intensity estimation when light is highly polarized, and propose figure of merits to visualize this phenomenon.

2 DATA AND NOISE MODEL

In the imaging system we consider, the scene is illuminated with totally polarized light. A first image X_i, $i \in [1, N]$ is formed with the fraction of light backscattered by the scene which is in the same polarization state as the incident light (please note that for the sake of simplicity, one-dimensional notation is used for images). A second image Y_i is formed with the fraction of light polarized orthogonally to the incident light. At each pixel i, the values X_i (Y_i) are expressed in terms of number of photoelectrons measured by the detector. In the following, we will assume that the images X_i (Y_i) are homogeneous, that is, the average number of photoelectrons is equal to m_X (m_Y) for all pixels i. If the imaged scene is com-

Received December 10, 2007; published January 21, 2008 ISSN 1990-2573

plex, this model can thus represent a region where the values of m_X (m_Y) is approximately constant. This hypothesis is classical and necessary to study the estimation precision. The mean numbers of photoelectrons can also be written as

$$m_X = \frac{I}{2}(1+P) \quad \text{and} \quad m_Y = \frac{I}{2}(1-P). \tag{1}$$

The variable $I = m_X + m_Y$ denotes the total intensity of the signal, and the variable P represents its DOP.

The photoelectrons generated by the backscattered fraction of illumination light will be called the *useful signal*. In addition to this signal, we assume that an average number of g_X (g_Y) electrons are also measured by the detector in the channel $X_i(Y_i)$. These electrons correspond to the sum of all possible sources of additive noise. Let us consider some possible sources of such additive noise. A first one is dark current, which is due to the generation of electrons in the detector in the absence of illumination. This noise depends mainly on temperature and exposure time, and is known to follow a Poisson distribution [10]. For such a noise, the parameters g_X (g_Y) represent the average number of dark electrons measured in each channel. Since images X_i and Y_i are measured by identical sensors in similar conditions, one has naturally the same average number of dark current electrons on both parallel and orthogonal channels, that is, $g_X = g_Y = g$.

A second type of noise is always encountered in active imagery systems, where the useful signal is due to the fraction of the polarized illumination which is backscattered by the scene. In general, there are also ambient light sources such as sun or lamps whose light is scattered by the scene and produce a signal whose quantum fluctuations can be considered as noise. Generally speaking, such light sources are unpolarized. Moreover, we consider that the materials that compose the scene can be considered totally depolarizing with good approximation [6]. Such materials have a diagonal Mueller matrix and thus have no polarizance [11]: if unpolarized light impinges on such materials, it remains unpolarized. One thus observes $g_X = g_Y = g$. To check this fact, we used an active imaging setup with a Basler A312f camera, and measured the contribution signals g_X and g_Y without active illumination in the two channels for different type of materials in the scene. It is seen in Table 1 that the difference between g_X and g_Y does not exceed 4%. This small difference can be due to orientation of the materials that may slightly polarize the light. In this setup, it can thus be assumed that $g_X = g_Y = g$. In infra-red imaging, another source of additive noise is thermal light emitted by the scene. If this light is unpolarized, it will generate an average number of photoelectrons g identical on both channels.

In this paper, we will limit ourselves to the case $g_X = g_Y = g$, since it contains most of the essential physical results. However, all the results obtained below can be easily generalized to the case $g_X \neq g_Y$ with a slight increase of complexity of the expressions. Finally, it is reasonably sound to assume that all the above mentioned sources of noise are independent. Since they all have Poisson statistics, their contributions are additive and the final value of g is the sum of the average number of photoelectrons related to each of these sources of noise.

Material	g_X	g_Y	$\frac{(g_X-g_Y)}{(g_X+g_Y)/2}$
white paper	395	409	3.5%
white teflon	1063	1069	0.5%
grey painting	1095	1140	4.0%
bare metal	1072	1062	0.9%

TABLE 1 Backscattered light (in Digital Unit) by different materials with unpolarized white ambient light. One has represented g_X, g_Y, and $\frac{(g_X-g_Y)}{(g_X+g_Y)/2}$ which represents the relative difference between g_X and g_Y.

Taking into account the photoelectrons from the useful signal and the additive noise, the average number of electrons measured by the detector in channel X_i (Y_i) is $m_X + g$ ($m_Y + g$). Associated with these average values are fluctuations, which are given by the Poisson statistics. The actual number of electrons n measured in channel U_i is thus a random variable distributed with the following probability law:

$$P_{U_i}(n) = \exp\left[-(m_U+g)\right] \frac{(m_U+g)^n}{n!}, \tag{2}$$

with $U = X$ or Y. According to this model, the fluctuations in channels X_i and Y_i are statistically independent.

3 PRECISION OF ESTIMATION OF INTENSITY AND DOP

Our objective is to determine the precision of estimation of the parameters I and P in the presence of the above defined fluctuations. For that purpose, we will determine the Cramer-Rao Lower Bound (CRLB), which is a lower bound on the variance that can be reached by unbiased estimators of these parameters, assuming that the parameter g is known. Determination of the CRLB first requires the expression of the log-likelihood [12]. According to the above defined statistical data model (see Eq. 2) and Eq. 1, the expression of the loglikelihood is:

$$\begin{aligned} \ell(I,P) &= \sum_{i=1}^{N} \log P_{X_i}(X_i) + \sum_{i=1}^{N} \log P_{Y_i}(Y_i) && (3)\\ &= -N(I+2g) + S_X \log\left[\frac{I}{2}(1+P)+g\right] \\ &\quad + S_Y \log\left[\frac{I}{2}(1-P)+g\right] + A, && (4) \end{aligned}$$

where A does not depend on I nor on P, $S_X = \sum_{i=1}^{N} X_i$ and $S_Y = \sum_{i=1}^{N} Y_i$. Using this expression, the Fisher matrix defined as $F = \left[-\left\langle \partial^2 \ell / (\partial\theta_i \partial\theta_j)\right\rangle\right]_{1\le i\le 2, 1\le j\le 2}$ where $\theta_1 = I$ and $\theta_2 = P$, has the following expression:

$$F = \frac{N}{Q}\begin{bmatrix} I(1-P^2)+2g(1+P^2) & 2gIP \\ 2gIP & I^2(I+2g) \end{bmatrix}, \tag{5}$$

where $Q = (I+2g)^2 - (IP)^2$. Taking the inverse of this matrix, one obtains:

$$J = F^{-1} = \frac{1}{N}\begin{bmatrix} I+2g & -2gP/I \\ -2gP/I & (1-P^2)/I + 2g(1+P^2)/I^2 \end{bmatrix}. \tag{6}$$

The parameters I and P can be gathered in a parameter vector $\mathbf{a}^T = (I, P)$. Let us consider an estimator $\widehat{\mathbf{a}}$ of the parameter vector $\mathbf{a}$, and assume that it is unbiased, that is, $\langle\widehat{\mathbf{a}}\rangle = \mathbf{a}_0$, where $\mathbf{a}_0$ is the true value of the parameters. The precision of this estimator can be characterized by its covariance matrix $\Gamma = \langle(\mathbf{a} - \mathbf{a}_0)(\mathbf{a} - \mathbf{a}_0)^T\rangle$. This covariance matrix is not easy to determine. The Cramer-Rao theorem provides a lower bound on the elements of this matrix in the following way [12]: $\forall \mathbf{v} \in \mathbb{R}^2, \mathbf{v}^T\Gamma\mathbf{v} \geq \mathbf{v}^T J\mathbf{v}$. In particular, if $\mathbf{v}$ is such that $v_i = 1$ and $\forall j \neq i$, $v_j = 0$, one obtains : $\Gamma_{ii} \geq J_{ii}$. Remembering that the diagonal element Γ_{ii} of the covariance matrix is equal to the variance of the component $\widehat{a}_i$ of the estimator, the matrix element J_{ii} represents a lower bound on the variance of unbiased estimation of parameter a_i, which is called Cramer-Rao Lower Bound (CRLB) [12].

Consequently, from the expression of J in Eq. 6, the CRLB κ_I and κ_P of I and P have the following expression:

$$\begin{aligned} \kappa_I(g) &= \kappa_I^{sd} + \kappa_I^a \\ &\text{with} \quad \kappa_I^{sd} = \frac{I}{N} \text{ and } \kappa_I^a = \frac{2g}{N}, \end{aligned} \tag{7}$$

$$\begin{aligned} \kappa_P(g) &= \kappa_P^{sd} + \kappa_P^a \\ &\text{with} \quad \kappa_P^{sd} = \frac{(1-P^2)}{NI} \text{ and } \kappa_P^a = \frac{2g(1+P^2)}{NI^2}. \end{aligned} \tag{8}$$

These expressions constitute the basic result of the present work. It is seen that for both estimations of I and P, the CRLB in the sum of the classical signal-dependent Poisson CRLB (κ_I^{sd}, κ_P^{sd}) and of a contribution due to the additive noise (κ_I^a, κ_P^a). Indeed, when the additive contribution to noise is zero, that is, $g = 0$, one has $\kappa_I(0) = \kappa_I^{sd} = I/N$, which is the well known value of the estimation variance of I in the presence of signal-dependent Poisson noise only. One also has $\kappa_P(0) = \kappa_P^{sd} = (1-P^2)/(NI)$, which has been shown in [8] to be the CRLB of DOP estimation in the presence of Poisson noise. The contribution of additive noise to intensity estimation is $\kappa_I^a = 2g/N$, which is simply the CRLB in the presence of the sum of two independent noises of variance g (one from the parallel channel and one from the orthogonal channel). The additive contribution to DOP estimation is $\kappa_P^a = 2g(1+P^2)/(NI^2)$. In [9], the CRLB in the presence of an additive Gaussian noise of variance σ^2 has been shown to be $2\sigma^2(1+P^2)/(NI^2)$. We can see a great similarity with κ_P^a, since the variance of the Poisson additive noise is g.

One can also note that the CRLB of I is independent of the actual DOP, P, whereas the CRLB of P depends on P. More precisely, κ_P^{sd} decreases with P and is null for totally polarized light. This is understandable since in this case, the average intensity in the orthogonal channel m_Y is 0 and thus the noise has also a zero variance in this channel. On the other hand, the additive contribution κ_P^a increases with P, and never reaches 0. Indeed, since the noise is independent of the intensity of the useful signal, it is always present even if the signal is zero.

4 COMPARISON OF ADDITIVE AND SIGNAL-DEPENDENT POISSON NOISES

It is of interest to analyze the influence of an increasing level of additive Poisson noises on the global estimation uncertainty. Let us first consider estimation of I. It is clear from Eq. 8 that the estimation variance increases with g. We have plotted in Figure 1 the ratio

$$\rho_I(g) = \frac{\kappa_I(g)}{\kappa_I(0)} = 1 + 2\frac{g}{I}, \tag{9}$$

which represents the ratio between the CRLB for a given value of g and the CRLB without additive noise, that is, $g = 0$. It increases linearly with the ratio g/I, which can be considered as a signal to noise ratio associated with the additive contribution to noise. Let us now consider estimation of the DOP. We have plotted on Figure 1 the ratio:

$$\rho_P(g) = \frac{\kappa_P(g)}{\kappa_P(0)} = 1 + 2\left(\frac{1+P^2}{1-P^2}\right)\frac{g}{I}. \tag{10}$$

This ratio also depends linearly on g/I, but the slope depends on the value of the DOP P. This slope tends to infinity as P tends to 1, that is, when light becomes highly polarized. It thus clearly appears that the influence of a given level of additive noise is higher on DOP estimation than on intensity estimation when light is highly polarized.

As another way of characterizing this effect, one can fix the parameter g and define "crossover" values of I that correspond to the situation where the CRLB corresponding to the signal-dependent and additive contributions are equal. This corresponds in Figure 1 to the intersections of the lines representing ρ_I and ρ_P and the horizontal line of equation $\rho = 2$. For intensity estimation, $\kappa_I^{sd} = \kappa_I^a$ is obtained when intensity is equal to:

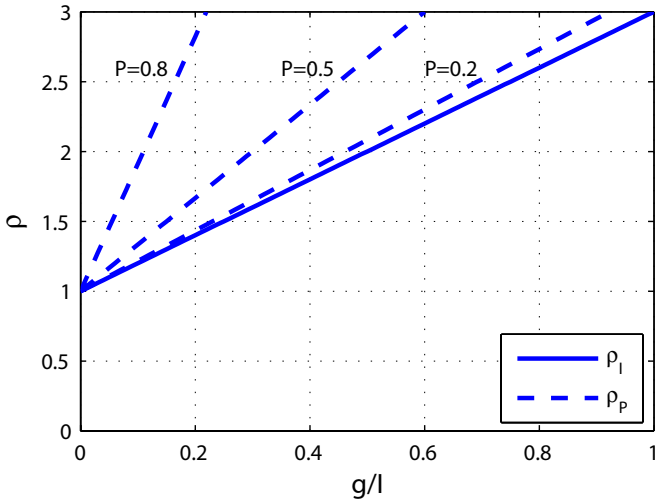

FIG. 1 Ratio $\rho_I(g)$ and $\rho_P(g)$ as a function of g/I for different values of P.

$$I_c^I = 2g,$$

that is, when the average intensity of the useful signal is twice that of the additive contribution. This value does not depend on the degree of polarization. When $I < I_c^I$, additive noise is dominant, whereas signal-dependent noise is dominant when $I > I_c^I$. Let us now consider estimation of P. The crossover happens when $\kappa_P^{sd} = \kappa_P^a$, that is, when intensity is equal to:

$$I_c^P = 2g\,\frac{1+P^2}{1-P^2}.$$

Contrary to the case of intensity estimation, this value depends on P. We have plotted in Figure 2 the ratio of the intensity and DOP crossover values I_c^P / I_c^I as a function of P. For totally depolarized light, one has $I_c^P = I_c^I$. On the other

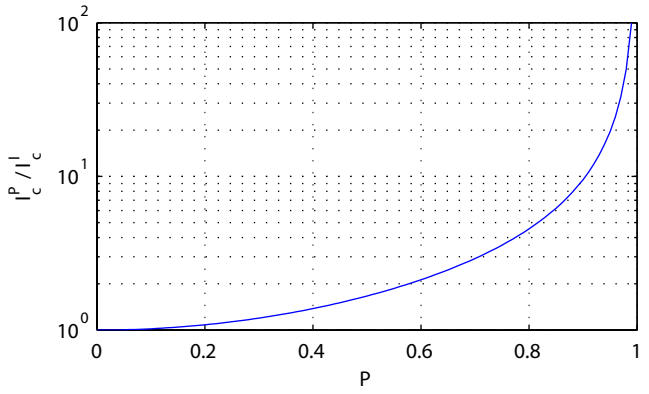

FIG. 2 Ratio I_c^P / I_c^I as a function of P.

hand, when P tends to 1, the ratio tends to infinity. For highly polarized light, I_c^P can thus be quite larger than I_c^I. For example, when $P = 0.9$, $I_c^P = 9.5\ I_c^I$. This means that to be limited by signal-dependent Poisson noise, one needs a number of photons which is 9 times larger than for intensity estimation. In other words, when light is highly polarized, additive noise must be taken into account for estimating the DOP even if it is negligible for intensity estimation.

To visualize the relative influence of the two sources of noise, it is useful to plot figures of merit. We have chosen to plot the noise variance as a function of the intensity of the useful signal with a log-log scale. For intensity estimation, one has: $\log_{10}[\kappa_I] = \log_{10}\left[\kappa_I^{sd} + \kappa_I^a\right]$. Below the crossover ($I < I_c^I$), the approximation is:

$$\log_{10}[\kappa_I] \simeq \log_{10}\left[\kappa_I^a\right] = -\log_{10}[2g] - \log_{10}[N], \qquad (11)$$

that is, a constant. Above the crossover, the approximation is:

$$\log_{10}[\kappa_I] \simeq \log_{10}\left[\kappa_I^{sd}\right] = \log_{10}[I] - \log_{10}[N], \qquad (12)$$

that is, an increasing line of slope equal to 1. This is the well known figure of merit for intensity estimation [10]. It is plotted in Figure 3 for $N = 1$. Increasing N only shifts the curve downwards of a value $-\log_{10}[N]$.

Let us now consider DOP estimation. One has $\log_{10}(\kappa_P) = \log_{10}\left[\kappa_P^{sd} + \kappa_P^a\right]$. Below the crossover, ($I < I_c^P$), an approximation is:

$$\log_{10}[\kappa_P] \simeq \log_{10}\left[\kappa_P^a\right] = -2\log_{10}[I] - \log_{10}[1+P^2] - \log_{10}[2g] - \log_{10}[N], \qquad (13)$$

that is, a decreasing line with slope 2. Above the crossover, an approximation is:

$$\log_{10}[\kappa_P] \simeq \log_{10}\left[\kappa_P^{sd}\right] = -\log_{10}[I] - \log_{10}[1-P^2] - \log_{10}[N], \qquad (14)$$

that is, an decreasing line with slope 1. We have plotted this curve in Figure 4 for $N = 1$ and different values of P. It is

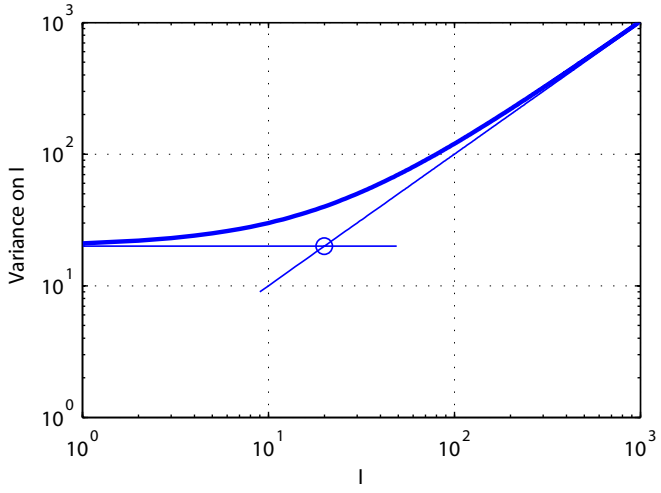

FIG. 3 Estimation precision of I as a function of the actual value of I, $g = 10$ photons, bold line : κ_I, dotted lines : κ_I^a and κ_I^{sd}, circle : crossover location(I_c^I).

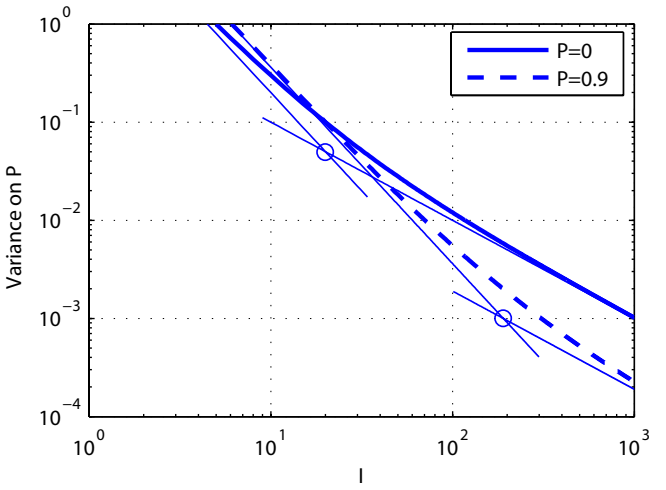

FIG. 4 Estimation precision of P as a function of the actual value of I, $g = 10$ photons, bold dotted line : κ_P for $P = 0$, bold continuous line : κ_P for $P = 0.9$, dotted lines : κ_I^a and κ_I^{sd}, circles : crossover locations(I_c^P).

seen that higher values of P lead to a significant shift of the crossover value.

The main result of this work is that the influence of additive Poisson noise on DOP estimation depends on the actual value of the DOP. When P is large, the additive Poisson noise remains dominant for much higher values of the mean photon flux. This result is important for processing of polarimetric images (estimation, target detection ...). Indeed, the algorithms used for extracting information from polarimetric images must be adapted to the dominant type of noise.

5 CONCLUSION

We have studied precision of DOP estimation when the observed materials are purely depolarizing and the measurements are perturbed with both signal-dependent and additive Poisson noises. This precision depends on the value of the DOP and, when light is highly polarized, the crossover

between additive and signal-dependent noise-dominant regimes occurs for significantly higher signal levels than for intensity estimation. This fact must be taken into account when designing algorithms for extracting information from DOP images. The present study is based on CRLB, which represents a potential estimation precision. An interesting perspective is to determine and analyze the performance of actual DOP estimators adapted to this noise model.

6 ACKNOWLEDGEMENTS

Arnaud Bénière's PhD thesis is supported by the Délégation Générale pour l'Armement (DGA), and followed by the Mission pour la Recherche et l'Innovation Scientifique (MRIS), domain IMAT (Jacques Blanc-Talon). The authors would also like to thank anonymous reviewers of the journal for valuable comments and suggestions for improvement of the manuscript.

References

[1] O. Matoba and B. Javidi, "Three-dimensional polarimetric integral imaging" Opt. Lett. **29**, 2375–2377 (2004).

[2] M. Alouini, F. Goudail, P. Réfrégier, A. Grisard, E. Lallier, and D. Dolfi, "Multispectral polarimetric imaging with coherent illumination: towards higher image contrast" in *Polarization: Measurement, Analysis, and Remote Sensing VI*, D. H. Goldstein and D. B. Chenault, eds. (Proc. SPIE, vol. 5432, pp. 133–144, 2004).

[3] S. L. Jacques, J. C. Ramella-Roman, and K. Lee, "Imaging skin pathology with polarized light" J. Biomed. Opt. **7**, 329–340 (2002).

[4] J. M. Bueno, J. Hunter, C. Cookson, M. Kisilak, and M. Campbell, "Improved scanning laser fundus imaging using polarimetry" J. Opt. Soc. Am. A **24**, 1337–1348 (2007).

[5] S. Jiao and L. V. Wang, "Two-dimensional depth-resolved Mueller matrix of biological tissue measured with double-beam polarization-sensitive optical coherence tomography" Opt. Lett. **27**, 101–103 (2002).

[6] S. Breugnot and P. Clémenceau, "Modeling and performances of a Polarization Active Imager at $\lambda = 806$ nm" Opt. Eng. **39**, 2681–2688 (2000).

[7] P. Réfrégier, F. Goudail, and N. Roux, "Estimation of the degree of polarization in active coherent imagery using the natural representation" J. Opt. Soc. Am. A **21**, 2292–2300 (2004).

[8] P. Réfrégier, M. Roche, and F. Goudail, "Cramer-Rao lower bound for the estimation of the degree of polarization in active coherent imagery at low photon level." Opt. Lett. **31**, 3565–3567 (2006).

[9] A. Bénière, F. Goudail, M. Alouini, and D. Dolfi, "Precision of degree of polarization estimation in the presence of additive Gaussian detector noise" Opt. Commun. **278**, 264–269 (2007).

[10] G. C. Holst, *CCD arrays, cameras, and displays, Second Edtion* (JCD Publishing, Winter Park, Florida, 1998).

[11] S. Y. Lu and R. A. Chipman, "Interpretation of Mueller matrices based on polar decomposition" J. Opt. Soc. Am. A **13**, 1106–1113 (1996).

[12] H. L. Van Trees, *Detection, Estimation and Modulation Theory*. (John Wiley and Sons, Inc., New York, 1968).